

Zero-point Renormalization of the Band Gap of Semiconductors and Insulators Using the PAW Method

Manuel Engel¹, Henrique Miranda², Laurent Chaput³, Atsushi Togo⁴,
Carla Verdi¹, Martijn Marsman¹, Georg Kresse¹

¹ University of Vienna, Austria ² VASP Software GmbH, Austria ³ LEMTA - Université de Lorraine, France
⁴ National Institute for Materials Science, Japan

Projector-Augmented-Wave (PAW) Method

Imagine that we solve the Kohn-Sham (KS) equations (at least we try). The resulting all-electron (AE) orbitals are represented using plane waves.

Problem

The AE orbitals are orthogonal to each other. Therefore, they exhibit rapid oscillations in proximity to the nuclei. An accurate description of this phenomenon requires numerous plane-wave coefficients. This incurs a high computational cost.

Solution

We transform the AE orbitals into computationally convenient pseudo (PS) orbitals^[2]. The PS orbitals are smoother and require fewer plane-wave coefficients, at the price of no longer being orthogonal.

$$|\psi_{nk}\rangle = \hat{T} |\tilde{\psi}_{nk}\rangle \quad \tilde{H} |\tilde{\psi}_{nk}\rangle = \varepsilon_{nk} \tilde{S} |\tilde{\psi}_{nk}\rangle \quad \tilde{S} = \hat{T}^\dagger \hat{T} \\ \tilde{H} = \hat{T}^\dagger \hat{H} \hat{T}$$

PAW Transformation PAW KS Equations PAW Operators

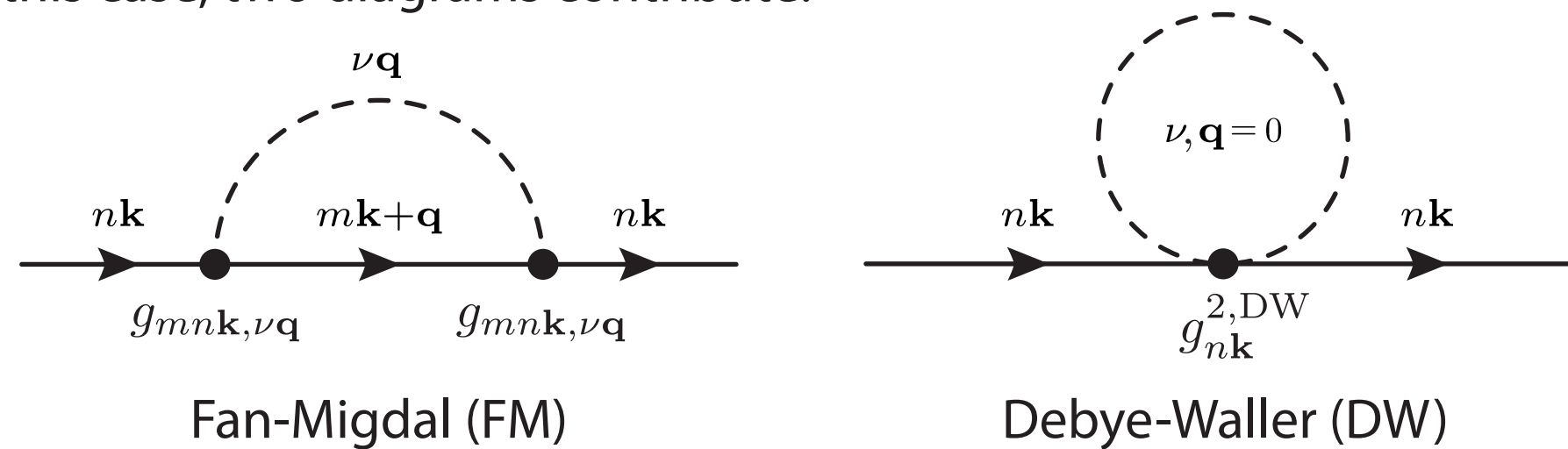
AE information is retained inside augmentation spheres around each nucleus using a radial basis set, the so-called partial waves, $|\phi_{ai}\rangle$ and $|\tilde{\phi}_{ai}\rangle$.

$$|\Psi_n\rangle = |\tilde{\Psi}_n\rangle - \sum_{ai} c_{nai} |\tilde{\phi}_{ai}\rangle + \sum_{ai} c_{nai} |\phi_{ai}\rangle$$

Finally, the wavefunction characters, c_{nai} , are calculated by projecting the PS orbitals onto PAW projector functions, $|\tilde{p}_{ai}\rangle$: $c_{nai} \equiv \langle \tilde{p}_{ai} | \tilde{\psi}_n \rangle$

Zero-Point Renormalization (ZPR)

When electrons couple with the vibrations of the crystal lattice (phonons), the Kohn-Sham eigenvalues become renormalized. At zero Kelvin, this is called zero-point renormalization. This is particularly important for the band gap. We use perturbation theory at lowest order to calculate the ZPR. In this case, two diagrams contribute:



$$\Delta \varepsilon_{nk}^{\text{FM}}(T=0) = \int_{\text{BZ}} \frac{d^3q}{\Omega_{\text{BZ}}} \sum_{\nu} \sum_m |g_{m\nu, \nu\mathbf{q}}|^2 \text{Re} \left[\frac{1}{\varepsilon_{nk} - \varepsilon_{m\mathbf{k}+\mathbf{q}} \pm \hbar\omega_{\nu\mathbf{q}} + i\delta} \right]$$

Problem

The ZPR needs to be converged with respect to the number of intermediate states and phonon momenta.

Solution

We use a Fourier-interpolation technique that combines the accurate Bloch states from the unit cell with the electron-phonon potential from a supercell. This way, we can systematically increase the number of states as well as the q-point density.

The DW term can be calculated similarly after employing the so-called rigid-ion approximation.

Electron-Phonon Matrix Element

The electron-phonon matrix element measures the coupling strength between electrons and phonons. It can be regarded as the probability amplitude associated with this fundamental scattering process:

$$g_{m\nu, \nu\mathbf{q}} \equiv \langle \psi_{m\mathbf{k}+\mathbf{q}} | \partial_{\nu\mathbf{q}} \hat{H} | \psi_{n\mathbf{k}} \rangle \\ \partial_{\nu\mathbf{q}} \equiv \sum_{l\kappa\alpha} \sqrt{\frac{\hbar}{2M_{\kappa}\omega_{\nu\mathbf{q}}}} e_{\kappa\alpha, \nu\mathbf{q}} e^{i\mathbf{q}\cdot\mathbf{R}_l} \partial_{l\kappa\alpha}$$

Recipe for calculating electron-phonon matrix elements^[4]:

- Calculate force constants and derivative of potential in supercell using **finite displacements**
- Fourier interpolate dynamical matrix to unit cell to obtain phonon **modes and frequencies**
- Fourier interpolate **electron-phonon potential** to unit cell
- Sandwich **electron-phonon potential** between **Bloch states** in unit cell

Problem

Polar materials exhibit long-range electrostatic interactions for longitudinal optical phonon modes. Fourier interpolation will fail in this case due to the long-range nature of the phenomenon.

Solution

We remove the long-range part of the potential due to dipole interactions before the Fourier interpolation and add it back afterwards. It has a simple analytic form:

$$\frac{\partial \tilde{v}_{\mathbf{R}_\kappa}^{\mathbf{q}}}{\partial \mathbf{R}_\kappa} = \frac{4\pi e^2}{\Omega} \sum_{\mathbf{G} \neq -\mathbf{q}} \frac{-i\mathbf{Z}_\kappa^* \cdot (\mathbf{q} + \mathbf{G}) e^{i(\mathbf{q} + \mathbf{G}) \cdot (\mathbf{r} - \mathbf{R}_\kappa)}}{(\mathbf{q} + \mathbf{G}) \cdot \epsilon_\infty \cdot (\mathbf{q} + \mathbf{G})}$$

\mathbf{Z}_κ^* ... Born-effective-charge tensor ϵ_∞ ... static dielectric tensor

We have two methods of calculating the ZPR. They are equivalent in the adiabatic limit if the rigid-ion approximation is not employed.

PS Method^[3]

$$\tilde{g}_{m\nu, \nu\mathbf{q}} \equiv \langle \tilde{\psi}_{m\mathbf{k}+\mathbf{q}} | \partial_{\nu\mathbf{q}} \tilde{H} - \varepsilon_{nk} \partial_{\nu\mathbf{q}} \tilde{S} | \tilde{\psi}_{n\mathbf{k}} \rangle$$

Advantages

- Fast ZPR convergence
- Easy to implement
- AE information is preserved implicitly

Disadvantages

- Formally only valid for adiabatic electron-phonon renormalization
- Expected to fail for other observables

AE Method^[4]

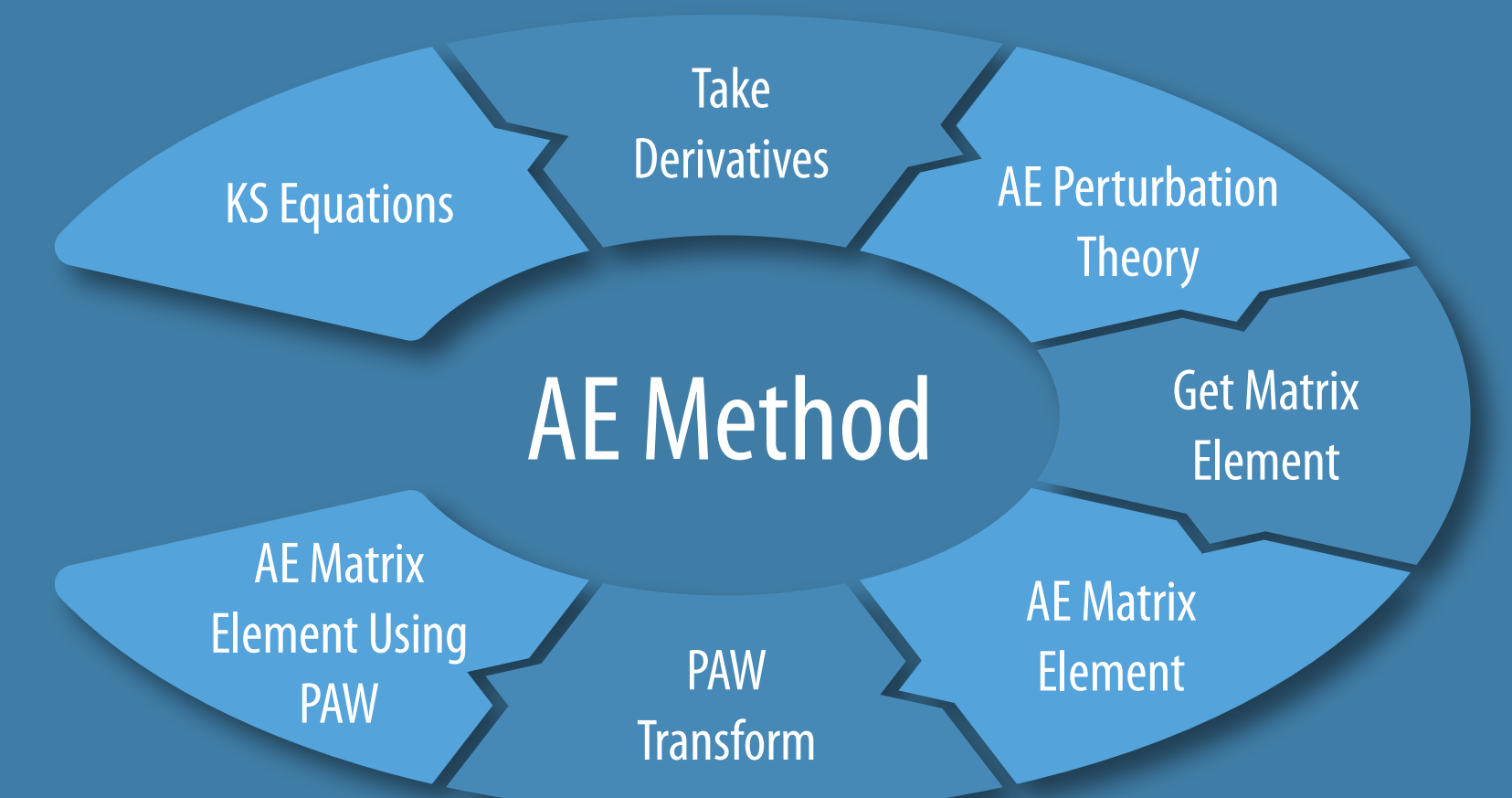
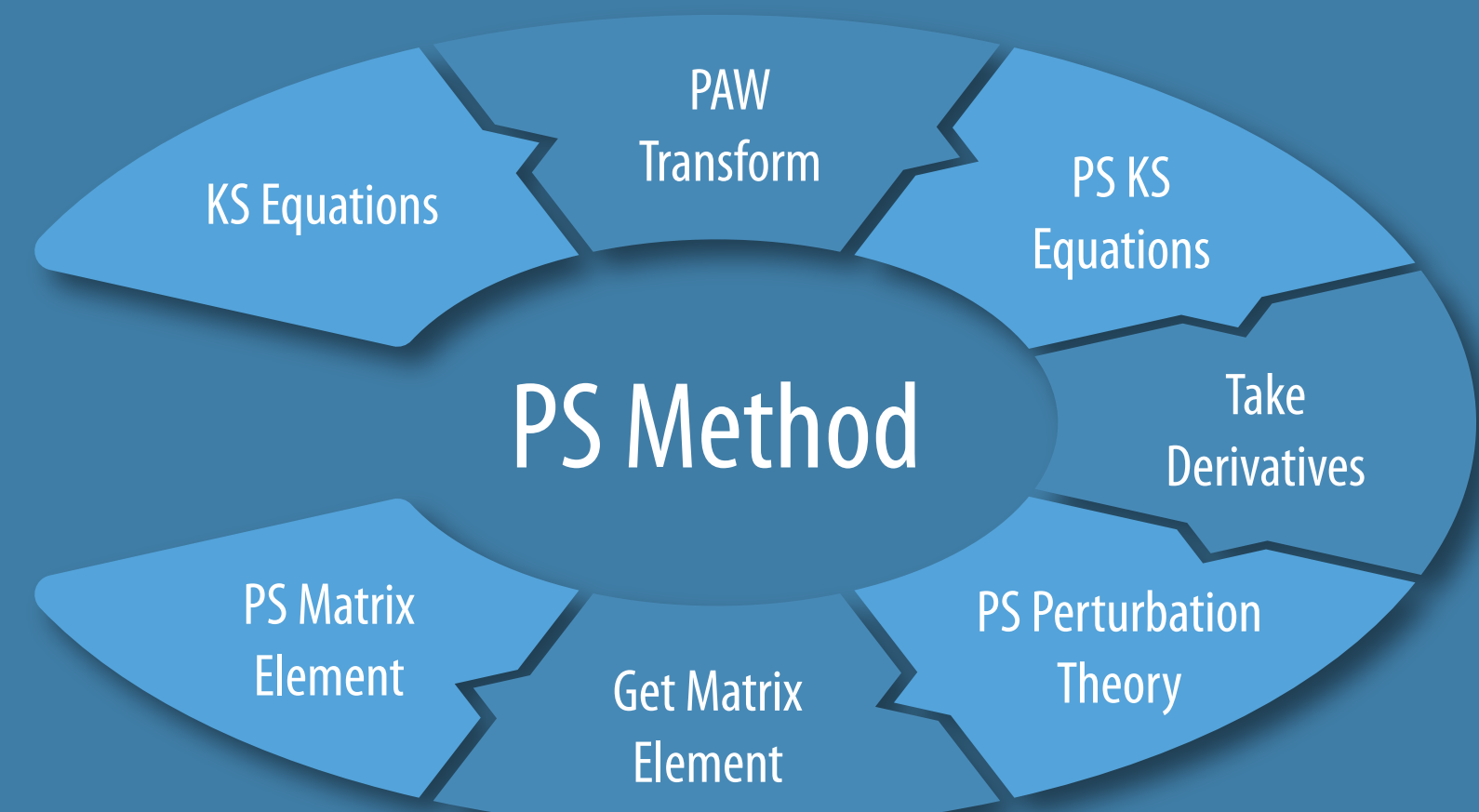
$$g_{m\nu, \nu\mathbf{q}} \equiv \tilde{g}_{m\nu, \nu\mathbf{q}} + (\varepsilon_{nk} - \varepsilon_{m\mathbf{k}+\mathbf{q}}) t_{m\nu, \nu\mathbf{q}} \\ t_{m\nu, \nu\mathbf{q}} \equiv \langle \tilde{\psi}_{m\mathbf{k}+\mathbf{q}} | \hat{T}^\dagger \partial_{\nu\mathbf{q}} \hat{T} | \tilde{\psi}_{n\mathbf{k}} \rangle$$

Advantages

- Equations unaffected by PAW transform
- Usable everywhere, not just for ZPR
- Full AE treatment of the coupling

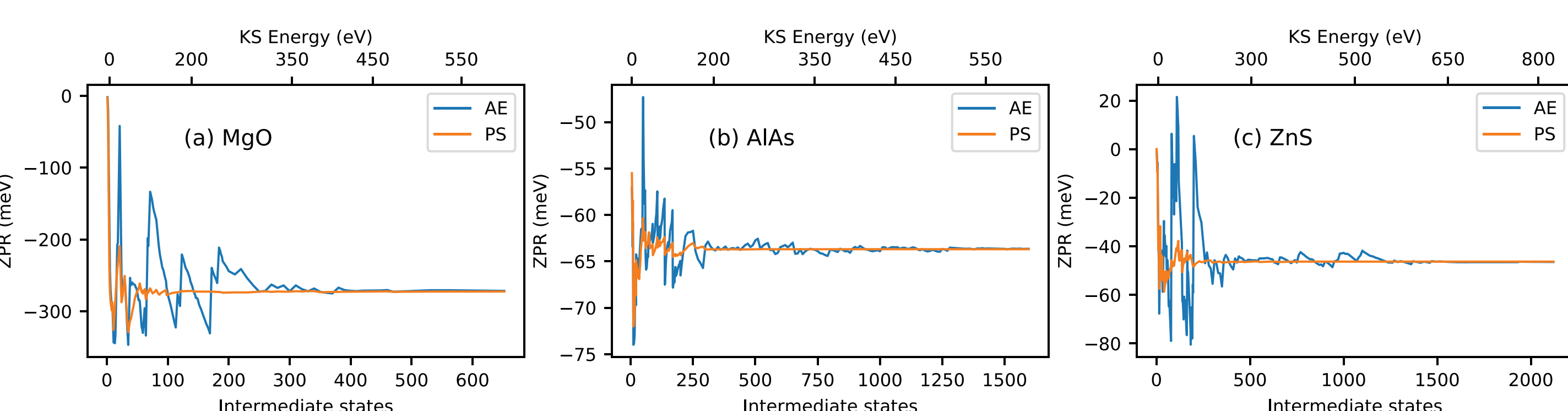
Disadvantages

- Slow ZPR convergence
- More dependent on pseudopotential
- More difficult to implement

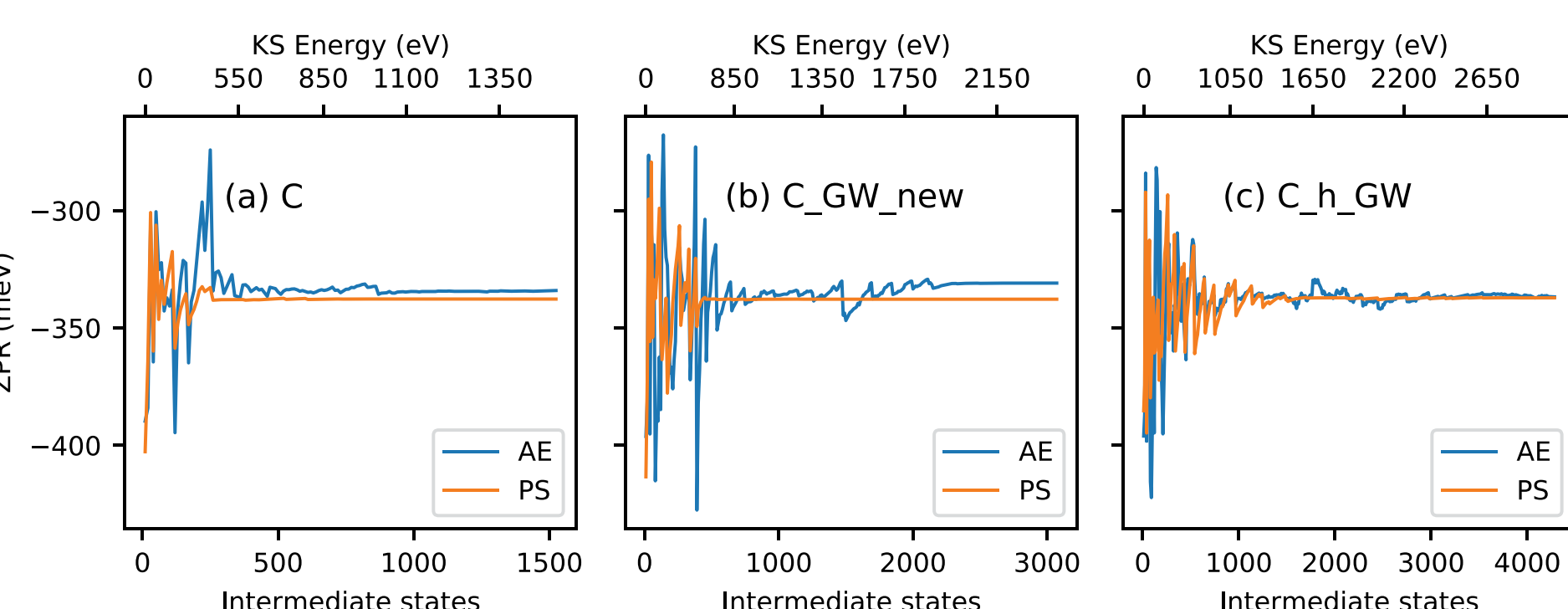


Results^[1]

AE and PS methods yield the same non-adiabatic band-gap ZPR for MgO, AlAs and ZnS. The AE approach requires significantly more intermediate states to converge.



In the case of diamond, the AE approach depends significantly on the pseudopotential used. Only after using the C_h_GW potential, which features a smaller core radius, did the AE and PS results coincide.



material	POTCAR	E_{cut} (eV)	ZPR AE	ZPR PS
AlAs-zb	Al As	600	-64	-64
C-cd	C	1500	-334	-338
C-cd	C_h_GW_new	2400	-331	-338
C-cd	C_h_GW	3000	-337	-337
MgO-rs	Mg O_s	600	-272	-273
ZnS-zb	Zn S	800	-46	-46

Non-adiabatic band-gap ZPR (meV) of various semiconductors and insulators compared against Literature. The obtained results are satisfactory.

material	ZPR this work	ZPR Ref. [5]	rel. diff.	abs. diff.
AlAs-zb	-74	-74	0.2%	0
AlN-w	-377	-399	5.5%	22
AlP-zb	-96	-93	2.9%	3
AlSb-zb	-52	-51	1.8%	1
BN-zb	-402	-406	0.9%	4
BaO-rs	-277	-271	2.4%	6
BeO-w	-726	-699	3.9%	27
C-cd	-323	-330	2.0%	7
CaO-rs	-357	-341	4.8%	16
CdS-zb	-67	-70	3.8%	3
CdSe-zb	-29	-34	15.2%	5
CdTe-zb	-19	-20	7.4%	1
GaN-w	-171	-189	9.5%	18
GaN-zb	-163	-176	7.6%	13
GaP-zb	-69	-65	5.7%	4
Li2O	-569	-573	0.6%	4
LiF-rs	-1231	-	-	-
MgO-rs	-533	-524	1.6%	9
Si-cd	-58	-56	4.1%	2
SiC-zb	-175	-179	2.1%	4
SiO2-t	-583	-585	0.4%	2
SnO2-t	-232	-215	7.9%	17
SrO-rs	-323	-326	1.0%	3
TiO2-t	-349	-337	3.5%	12
ZnO-w	-175	-157	11.2%	18
ZnS-zb	-88	-88	0.2%	0
ZnSe-zb	-43	-44	3.1%	1
ZnTe-zb	-25	-22	14.4%	3

Conclusion

We have implemented a state-of-the-art algorithm in VASP for calculating the electron self-energy using finite differences and the PAW method. This provides access to the phonon-induced renormalization of the electronic bandstructure, as well as other quantities.

In this work, we demonstrated the current capabilities of the code and compared against literature values. We have compared two approaches to calculating electron-phonon matrix elements and explored their respective advantages. Based on our limited experience with ZPR calculations, we found that the PS approach converges to the same result as the AE approach. In addition, it converges faster and is more robust with respect to the choice of pseudopotential.

Future Developments

- Add more electron-phonon features
 - Transport
 - Phonon self-energy
 - Eliashberg function
 - Spin-orbit coupling
 - Dynamic quadrupoles in the long-range part
- Compare AE and PS approaches for other observables
- Extend PS formalism beyond electron-phonon renormalization

[1] M. Engel, H. Miranda, L. Chaput, A. Togo, C. Verdi, M. Marsman, and G. Kresse, *Zero-Point Renormalization of the Band Gap of Semiconductors and Insulators Using the PAW Method*, arXiv:2205.04265 (submitted).

[2] G. Kresse, and D. Joubert, *From ultrasoft pseudopotentials to the projector augmented-wave method*, Phys. Rev. B 59, 1758–1775 (1999).

[3] M. Engel, M. Marsman, C. Franchini, and G. Kresse, *Electron-phonon interactions using the projector augmented-wave method and Wannier functions*, Phys. Rev. B 101, 184302 (2020).

[4] L. Chaput, A. Togo, and I. Tanaka, *Finite-Displacement Computation of the Electron-Phonon Interaction within the Projector Augmented-Wave Method*, Phys. Rev. B 100, 174304 (2019).

[5] A. Miglio, V. Brousseau-Couture, E. Godbout, G. Antonius, Y.-H. Chan, S. G. Louie, M. Côté, M. Giantomassi, and X. Gonze, *Predominance of non-adiabatic effects in zero-point renormalization of the electronic band gap*, npj Computational Materials 6, 167 (2020).

